Executive Summary

*E*nergy Dependence of Dispersive effects in Unpolarized Inclusive Elastic Electron/Positron-Nucleus Scattering

P. Guèye[1] (Spokesperson); D. Higinbotham[2] (Co-Spokesperson); J. Arrington[3] (Co-Spokesperson); P. Giuliani[1] (Co-Spokesperson), A. A. Kabir[4], E. Voutier[5]

[1]*Facility for Rare Isotope Beams, Michigan State University, East Lansing, MI, USA*
[2]*Thomas Jefferson National Accelerator Facility, Newport News, VA, USA*
[3]*Lawrence Berkeley National Laboratory, Berkeley, CA, USA*
[4]*Hampton University, Hampton, VA, USA*
[5]*Université Paris-Saclay, Orsay, France*

Measurements of elastic electron scattering data within the past decade have highlighted two-photon exchange contributions as a necessary ingredient in theoretical calculations to precisely evaluate hydrogen elastic scattering cross sections. This correction can modify the cross section at the few percent level. In contrast, dispersive effects can cause significantly larger changes from the Born approximation. A recent analysis of the ^{12}C elastic cross section around the first diffraction minimum [1], where the Born term contributions to the cross section are small to maximize the sensitivity to dispersive effects, was performed using the JLab LEDEX data from the high resolution Jefferson Lab Hall A spectrometers at beam energies of 362 MeV and 685 MeV. The results are in very good agreement with previous world data, although with less precision. The average deviation from a static nuclear charge distribution expected from linear and quadratic fits indicate a 30.6% contribution of dispersive effects to the cross section at 1 GeV. The magnitude of these effects near the first diffraction minimum of ^{12}C has been confirmed to be large with a strong energy dependence and could account for a large fraction of the magnitude for the observed quenching of the longitudinal nuclear response. These effects could also be important for nuclear radii extracted from parity-violating asymmetries measured near a diffraction minimum. The authors concluded it was important that a systematic study of the dispersion corrections inside and outside diffraction minima for a large range of (light through heavy) nuclei be performed using both unpolarized and polarized beams/targets to help provide a more complete understanding of elastic (and inelastic) electron/positron-nucleus scattering.

This Letter Of Intent (LOI) is submitted to present the case to measure the magnitude of the dispersive effects through electron and positron inclusive $\mathrm{A}(\mathrm{e},\mathrm{e}')$ *elastic scattering around the first diffraction minimum of several nuclei (*^{12}*C,* ^{27}*Al,* ^{29}*Cu,* ^{48}*Ca,* ^{56}*Fe, and* ^{208}*Pb) at five incident beam energies (0.55, 1.1, 2.2, 3.3 and 4.4 GeV) in either the experimental Hall A or C at Jefferson Lab.* ***These measurements will consist of the first ever comprehensive study of the energy dependence of these effects.***

Contents

A. Physics motivation

1. Introduction

During the 80s and 90s, higher order corrections to the first Born approximation were extensively studied through dedicated elastic and quasi-elastic scattering experiments using unpolarized electron and positron beams (see [2, 3, 4, 5, 6, 7] and references therein), following the seminal paper from [8]. These effects scale as $S_{HOB} = V_C/E_e$ where S_{HOB} is the scaling factor to account for higher order corrections to the Born approximation, V_C is the Coulomb potential of the target nucleus and E_e is the incident energy of the lepton probe [7]. Incidentally, they are expected to be small in the medium to intermediate energy regime, and have been neglected in the analysis of GeV energy data: V_C reaches a maximum of about 26 MeV for ^{208}Pb with a corresponding value of $S_{HOB} = 0.52\%$ for a 5 GeV beam.

In the 1$^{\text{st}}$ order approximation, the scattering cross section is evaluated using plane wave functions for the incoming and outgoing electrons. This approach is also known as the Plane Wave Born approximation (PWBA) or simply the Born Approximation (Fig. 1). Coulomb corrections originate from the Coulomb field of the target nucleus that causes an acceleration (deceleration) of the incoming (outgoing) electrons and a Coulomb distortion of the plane waves: these effects are treated within a Distorted Wave Born Approximation (DWBA) analysis for inelastic scattering or elastic/quasi-elastic scattering on heavy nuclei [7]. Two other corrections are required to properly evaluate the scattering cross section: radiative corrections due to energy loss processes and dispersive effects due to virtual excitations of the nucleus at the moment of the interaction (Fig. 1).

Within the last decade, a renewed interest arose from a discrepancy between unpolarized and polarized elastic scattering data on the measurement of the proton form factor ratio $\mu G_E^p/G_M^p$ which can be attributed to the contribution of two-photon exchanges [9, 10, 11, 12, 13, 14, 15, 16]. These effects have been investigated with a series of dedicated experiments [17, 18, 19, 20] (also see reviews [21, 22, 23] and references therein), including their impact on the measurement of form factors for nucleons and light ($A \leq 3$) nuclei. They include both Coulomb corrections [7, 24], excited intermediate states and treatment of the off-shell nucleons through dispersion relations as a function of the 4-momentum transfer.

Coulomb corrections have historically been labeled as *static* corrections to the Born approximation as depicted in Fig. 1. While these effects contribute to a few percents [7, 21, 22, 24], *dynamic* corrections known as dispersive effects are emphasized in the diffraction minima, where the first-order (Born approximation) cross section has a zero, and can contribute up to 18% in the first diffraction minimum of ^{12}C at 690 MeV [5, 6].

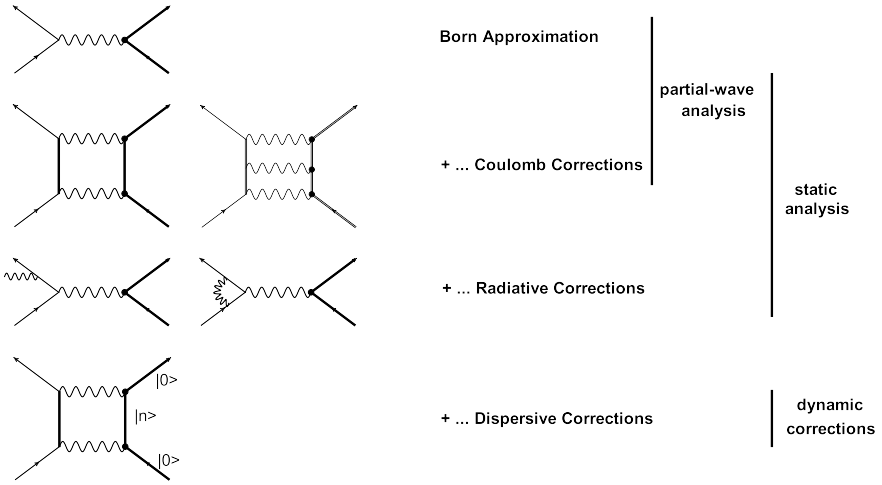

Figure 1: High-order corrections to the one-photon exchange Born approximation in electron/positron-nucleus scattering.

The electromagnetic nuclear elastic cross section for electrons can be expressed as:

$$\frac{d\sigma}{d\Omega} = \left(\frac{d\sigma}{d\Omega}\right)_{Mott} \mid F(q^2) \mid^2 \tag{1}$$

where $\left(\frac{d\sigma}{d\Omega}\right)_{Mott}$ is the Mott cross section corresponding to the scattering on a point-like nuclear target, $F(q^2)$ represents the form factor and $q^2 = -Q^2$ is the 4-momentum transfer.

Theoretical calculations for dispersive effects in elastic electron scattering for p-shell, spin-0 targets such as ^{12}C were performed in the mid-70s by Friar and Rosen [25]. They used a harmonic oscillator model and only the longitudinal (Coulomb) component to calculate the scattering amplitude within the PBWA approximation; the transverse component was neglected. The matrix element in the center-of-mass frame – considering only the contribution from the dominant two photon exchange diagrams – can be written as:

$$\mathcal{M}_{disp} = \sum_{n\neq 0} \int \frac{d^3\vec{p}}{\vec{q}_1^2 \vec{q}_2^2} \frac{\langle 0|\rho(\vec{q}_2)|n\rangle \langle n|\rho(\vec{q}_1)|0\rangle}{p^2 - p_n^2 - i\varepsilon} a(p_n) \tag{2}$$

with:

$$\left\{ \begin{array}{lcl} a(p_n) & = & E_e p_n [1 + \cos\theta] + \vec{p} \cdot (\vec{p_e} + \vec{p}_{e'}) \\ p_n & = & E_e - \omega_n - \frac{p^2 - E_e^2}{2M_p} \\ p & = & p_e - p_{e'} \end{array} \right. \tag{3}$$

where: $p_e = (E_e, \vec{p}_e)$ and $p_{e'} = (E_{e'}, \vec{p}_{e'})$ the 4-momentum of the incoming and outgoing electrons, respectively, and $\vec{q}_{1,2}$ the 3-momenta of the two photons exchanged. θ is the angle between the incoming and outgoing electrons. $\rho(\vec{q}_1)$ and $\rho(\vec{q}_2)$ are the charge operators associated with the two virtual photons, respectively, and using the notation of [25] with $\hat{e}_i(\vec{q})$ the charge distribution (operator in the isospin space) of the i$^{\text{th}}$ nucleon, gives:

$$\left\{ \begin{array}{lcl} \rho(\vec{q}) & = & \sum_{i=1}^{A} \hat{e}_i(\vec{q}) e^{i\vec{q}\cdot\vec{x'}_i} \\ \\ \hat{e}(\vec{q}) & = & \int \hat{e}(\vec{x}) e^{i\vec{q}\cdot\vec{x}} d^3\vec{x} \end{array} \right. \tag{4}$$

In their calculation, Friar and Rosen [25] also considered that all nuclear excitation states $|n\rangle$ have the same mean excitation energy ω, allowing to apply the closure relation: $\sum |n\rangle \langle n| = 1$. Including the elastic scattering and dispersion corrections leads to:

$$\mathcal{M}_{elast+disp} = (\alpha Z)F(q^2) + (\alpha Z)^2 G(q^2) \tag{5}$$

with $G(q^2)$ arising from two-photon exchange diagrams (including cross-diagram, seagull ...). Hence:

$$\begin{aligned} |\mathcal{M}_{elast+disp}|^2 &= (\alpha Z)^2 \big[F(q^2)\big]^2 \\ &+ 2(\alpha Z)^3 \big[F(q^2)\mathcal{R}e\{G(q^2)\}\big] \\ &+ (\alpha Z)^4 \big[|\mathcal{R}e\{G(q^2)\}|^2 + |\mathcal{I}m\{G(q^2)\}|^2\big] \end{aligned} \tag{6}$$

Therefore, the scattering amplitude is governed by $F(q^2)$ and the real part of $G(q^2)$ outside the minima of diffraction (where $F(q^2) \neq 0$). The imaginary part of $G(q^2)$ is most important in the minima of diffraction where the term $F(q^2)$ goes to zero.

Experimentally, in order to extract the magnitude of the dispersive effects, the momentum transfer q is modified to account for the Coulomb effects into an effective momentum transfer q_{eff} (we refer the reader to [7, 24, 26] for the validity of this so-called Effective Momentum Approximation). The latter is obtained by modifying the incident (E_e) and scattered ($E_{e'}$) energies of the incoming and outgoing electrons [7]:

$$q = 4E_e E_{e'} \sin^2(\theta/2) \rightarrow q_{eff} = 4E_{e,eff} E_{e',eff} \sin^2(\theta/2) \tag{7}$$

with $E_{e,eff} = E_e\Big(1 - \frac{|V_C|}{E_e}\Big)$ and $E_{e',eff} = E_{e'}\Big(1 - \frac{|V_C|}{E_e}\Big)$. $|V_C|$ is the (magnitude of the) Coulomb potential of the target nucleus. The corresponding experimentally measured cross section can then be compared to the theoretical cross section calculated using a static charge density [5].

2. The JLab LEDEX experiment

The Low Energy Deuteron EXperiment (LEDEX) [27] was performed in two phases: first in late 2006 with a beam energy of 685 MeV and then in early 2007 with a beam energy of 362 MeV. They both used a 99.95 % pure ^{12}C target with a density of 2.26 g/cm^3 and a thickness of 0.083 ± 0.001 g/cm^2. The combined momentum transfer range was $0.4 - 3.0$ fm^{-1}.

The kinematics of the LEDEX experiment inside the first diffraction minimum of ^{12}C correspond to 4-momentum transfers q of 1.85 fm^{-1} and 1.82 fm^{-1} (q_{eff} of 1.82 fm^{-1} and 1.81 fm^{-1}) for (362 MeV, 61°) and (685 MeV, 30.5°), respectively [28]. The measured elastic cross sections are found to be: $(3.26 \pm 0.28) \times 10^{-8}$ fm^2/sr for 362 MeV and $(2.35 \pm 0.11) \times 10^{-7}$ fm^2/sr for 685 MeV. They were compared to static cross sections calculated from a Fourier-Bessel (FB) parameterization extracted from the LEDEX data that is found to be almost identical to the one from Offermann et al. [5] and the agreement is within 0.1%.

The results of this analysis are compared to the world data on the left panel of Fig. 2. Note that σ^{FB}_{stat} is replaced by σ_{stat} to keep the text coherent throughout this document. From a first order (solid line) and a second order (dashed line) polynomial fits,extrapolations indicate deviations at 1 GeV of 28.9% and 32.2%, respectively (average of 30.6%). One pseudo-data point from the average of the fit functions is also shown at 1 GeV with a 3% error bar (which is a reasonable systematic error for an elastic peak cross section measurement at Jefferson lab for this energy). The theoretical prediction from Friar and Rosen [25] on the size of dispersive effects in the first diffraction minimum of ^{12}C is shown in the right panel of Fig. 2 for 374.5 MeV and 747.2 MeV

where the inclusion of dispersive corrections $\sigma_{stat+disp}$ is compared to the cross section σ_{stat} obtained from a static charge distribution: the expected (constant) 2% predicted discrepancy is clearly not reproducing the magnitude and energy dependence behavior seen in the data.

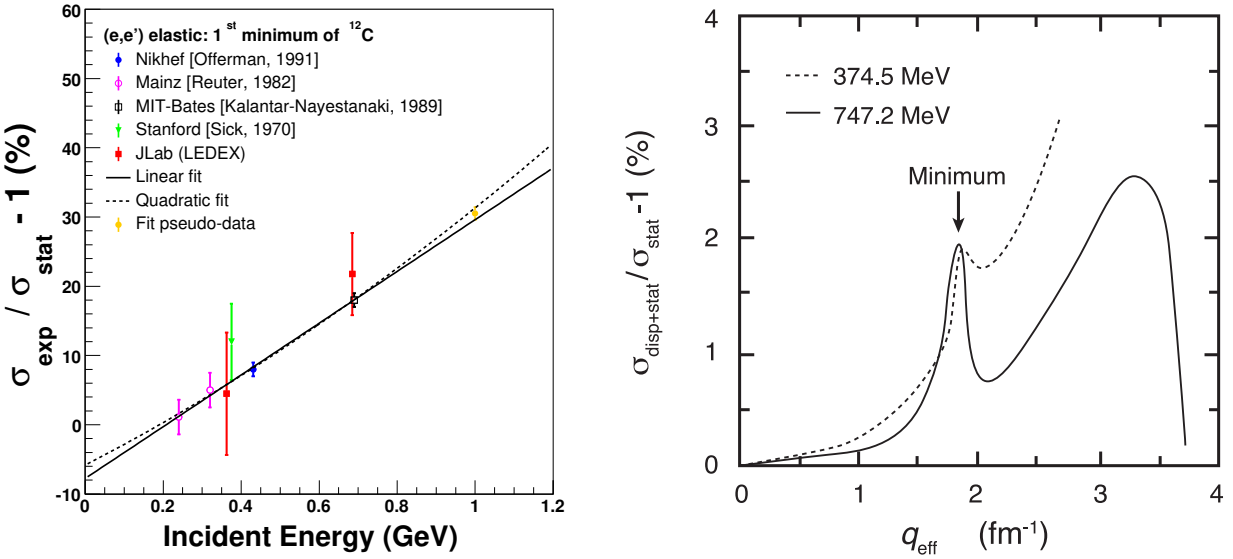

Figure 2: Left panel – World data on the energy dependence of dispersive effects in the first diffraction minimum of ^{12}C. In the y-axis, σ^{FB}_{stat} was replaced by σ_{stat} to keep coherency in the text. The first minimum at $q_{eff} = 1.84$ fm^{-1} moves slightly with beam energy as noted in [29] (this dependency is out of the scope of this paper). Right panel – Calculations of Friar and Rosen [25] for dispersion corrections to elastic electron scattering from ^{12}C at 374.5 and 747.2 MeV in the first diffraction minimum $q_{eff} = 1.84$ fm^{-1}.

3. Dispersive corrections and the nuclear matter

A very simplistic approach was used by the authors of [1] to estimate the effects of dispersive corrections on the nuclear charge density [30, 31] and the Coulomb Sum Rule [32].

Coulomb corrections stem from multi-photons exchange between the incoming lepton probe and the target nucleus, with 2γ being the dominant contribution from higher powers of the $Z\alpha$ terms (with the electromagnetic coupling constant $\alpha = 1/137$). To accurately estimate these effects, one should take into account the continuous change of the incident beam energy while the particle is approaching the nucleus. In practice, one assumes a constant Coulomb field to estimate these effects and applies an effective global shift of the incident and outgoing beam energies as described in Section A.1. Note that one should use the averaged Coulomb potential $|V_C| = \int \rho(r)|V_C|(r)d^3r/Z|e|$ instead of the potential at the origin of the nucleus $|V_C(0)|$ [7].

The dispersive cross section $\sigma_{disp} = \sigma_{stat+disp}$ (for simplicity) can be expressed as a function of the cross section σ_{stat}:

$$\sigma_{disp} = \sigma_{stat}[1 + \delta_{disp}(E_e)] \tag{8}$$

with $\delta_{disp}(E_e)$ the higher order correction to the Born Approximation. Our convention throughout the text is to label any quantity with the subscript *disp*, such as the cross section σ_{disp}, that has been directly obtained from experimental measurements and is affected by the contribution from dispersive effects. Analogously, the subscript *stat*, such as σ_{stat}, is attached to any quantity that could be obtained by removing the contribution from dispersive effects, thus correcting the

experimental observation. In that sense σ_{stat} will be the expected cross section from the Born Approximation. Equation (8) states that the observed experimental cross sections σ_{disp} could be modeled by a small multiplicative perturbation added to the static σ_{stat} cross section.

4. Effects on nuclear radii

In the Plane Wave Born Approximation, the nuclear charge density distribution $\rho_{\rm ch}(r)$ is the Fourier transform of the nuclear form factor and for spherically symmetric charge distributions the relation is [33]:

$$\rho_{\rm ch}(r) = \frac{1}{2\pi^2}\int F_{\rm ch}(q)\frac{\sin(qr)}{qr}q^2 dq \tag{9}$$

$\rho_{\rm ch}(r)$ can thus be extracted from the experimentally measured $F_{\rm ch}(q^2)$ and it is usually normalized to either 1 or the total charge of the nucleus. We adopt the first convention in this work:

$$4\pi\int \rho_{\rm ch}(r)r^2 dr = 1 \tag{10}$$

A model independent analysis can be done to extract the nuclear charge density distributions using either a sum of Gaussian (SOG) [34] or sum of Bessel (FB) [35] functions. We will only focus on the latter and refer the readers to reference [33] for more details on the former.

One can use the zero'th spherical Bessel function $j_0(r) = \sin(qr)/qr$ to expand the charge density as:

$$\rho^{\rm FB}_{\rm ch}(r) = \begin{cases} \sum_\nu a_\nu j_0\left(\frac{\nu\pi r}{R_{\rm cut}}\right) & \text{for} \quad r \le R_{\rm cut} \\ \\ 0 & \text{for} \quad r > R_{\rm cut} \end{cases} \tag{11}$$

with $R_{\rm cut}$ the cut-off radius chosen such as the charge distribution is zero beyond that value ($R_{\rm cut}$ = 8 fm for ^{12}C [5]) and the coefficients a_ν related to the form factor as $a_\nu = q_\nu^2 F_{\rm ch}(q_\nu)/2\pi R_{cut}$, where $q_\nu = \nu\pi/R_{cut}$ is obtained from the ν-th zero of the Bessel function j_0.

In this study we will ignore the contribution of the neutrons to the electric charge distribution of the nucleus[1]. Therefore, $\rho_{\rm ch}(r)$ could be considered as resulting from folding the distribution $\rho_{\rm nuc}(r)$ of the nucleons, protons in our approximation, inside the nucleus with the finite extension of the protons $\rho_p(r)$ [35]. The Fourier transform of $\rho_{\rm ch}(r)$ is then given by the product of the transform of $\rho_{\rm nuc}(r)$ and $\rho_p(r)$:

$$F_{\rm ch}(q) = F_{\rm nuc}(q)F_p(q) \tag{12}$$

The relationship between the corresponding radii is:

$$R^2_{\rm ch} = R^2_{\rm nuc} + R^2_p \tag{13}$$

with $R_p = 0.8414(19)$ fm the proton radius [36]. The rms $\langle r^2_{\rm ch}\rangle^{1/2}$ can then be obtained from the nuclear charge density distribution ($\rho_{\rm ch}$) which extends up to $R_{\rm cut}$. Its general expression is:

$$\langle r^2_{\rm ch}\rangle = \int_0^{R_{\rm cut}} \rho_{\rm ch}(r)r^2 d^3r = 4\pi\int_0^{R_{\rm cut}} \rho_{\rm ch}(r)r^4 dr \tag{14}$$

Using the Bessel expansion of $\rho_{\rm ch}$ from Eq. (11) leads to:

$$\langle r^2_{\rm ch}\rangle = 4\pi\int_0^{R_{\rm cut}} \sum_\nu a_\nu j_0\left(\frac{\nu\pi r}{R_{\rm cut}}\right) r^4 dr \tag{15}$$

[1] Even though the neutron has a total electric charge of zero, its charge density $\rho_n(r)$ is not zero. Nevertheless, its contribution to the total charge density of the nucleus is small.

Evaluating the integral of the Bessel function gives:

$$\int_0^{R_{cut}} j_0\left(\frac{\nu\pi r}{R_{cut}}\right) r^4 dr = \frac{(-1)^\nu R_{cut}^5 (6-\nu^2\pi^2)}{\nu^4\pi^4} \tag{16}$$

Substituting into Eq. (14):

$$\langle r_{\rm ch}^2\rangle = 4\pi \sum_\nu a_\nu \frac{(-1)^\nu R_{\rm cut}^5 (6-\nu^2\pi^2)}{\nu^4\pi^4} \tag{17}$$

Therefore, all the coefficients a_ν of the Fourier Bessel expansion play a role in estimating the radius of the charge density distribution, decreasing in importance as $1/\nu^2$. If the measured cross sections used to extract the value of the form factor $F_{\rm ch}(q)$ are indeed modified by the dispersive corrections, then the change would propagate through the fitted coefficients a_ν to the estimate of the charge radius $R_{\rm ch} \equiv \langle r_{\rm ch}^2\rangle^{1/2}$. The total change in $R_{\rm ch}$ can be written as [1]:

$$\delta R_{ch} = \sum_i^N \frac{\partial R_{ch}}{\partial y_i}\delta y_i = \sum_i^N \Big(\sum_\nu^M \frac{\partial R_{ch}}{\partial a_\nu}\frac{\partial a_\nu}{\partial y_i}\Big)\delta y_i, \tag{18}$$

where δy_i is the change in the i$^{\rm th}$ value of the form factor $y_i = F(q_i)$, in this case due to the dispersive effects. Estimating the exact values of δy_i is a complicated task beyond our scope since the change in the cross section as shown in Eq. (8) depends on the energy, but the momentum transfer q is a function of both the energy and the angle θ. Therefore, for the same fixed value of q we could have different pairs of (E, θ) which will be impacted differently.

In order to simplify our discussion, we assume that we can separate the total effect of the dispersive effects on the form factor values as:

$$F_{disp}(q) = F(q)_{stat}[1 + \frac{1}{2}\delta(E_e)S(q)], \tag{19}$$

with $\delta_{disp} = \delta(E_e)S(q)$ from Eq. (8) where $\delta(E_e)$ controls the overall strength of the perturbation and $S(q)$ controls the impact this change would have on different q values. The factor of $1/2$ comes from assuming that $\delta(E_e)$ is small and propagating the change from Eqs. (1) and (8): $F \propto \sqrt{\sigma}$ which implies $\delta F/F \propto (1/2)\ \delta\sigma/\sigma$.

Since the variable q depends on both E_e and θ, a separation such as Eq. (19) might not be completely accurate. As it can be seen in the calculations of Friar and Rosen (Fig. 2, right panel), a change in E_e clearly affects the overal shape of the dispersion corrections as a function of q. Nevertheless, Eq. (19) is simple enough to allow providing an estimate for the impact of such a change in inferred nuclear properties of the nucleus. In particular, we can write the change in the charge radius as:

$$R_{\rm ch}^{disp} = R_{\rm ch}^{stat}\left[1 + \beta\delta(E_e)\right]. \tag{20}$$

where β is a proportionality coefficient fixed once $S(q)$ is specified (e.g., for a given fixed strength $\delta(E_e)$, the change in the radius will depend on the shape of $S(q)$, which is encoded in β).

Figure 3 shows the results for three different test perturbations $S(q)$ plus an empirical one, when using the data without dispersive corrections from Offermann [5] (Table X) for the central values of the form factor [1]. For the three test cases these values were modified assuming a constant high value of $\delta(E_e) = 30\%$. The forms for $S(q)$ were divided into two categories: δ_4 and δ_5 represent up-shift of 1 (e.g., 15% when multiplied by 1/2 $\delta(E_e)$) on the value of $F(q_\nu)$ for $\nu = 4$ and $\nu = 5$,

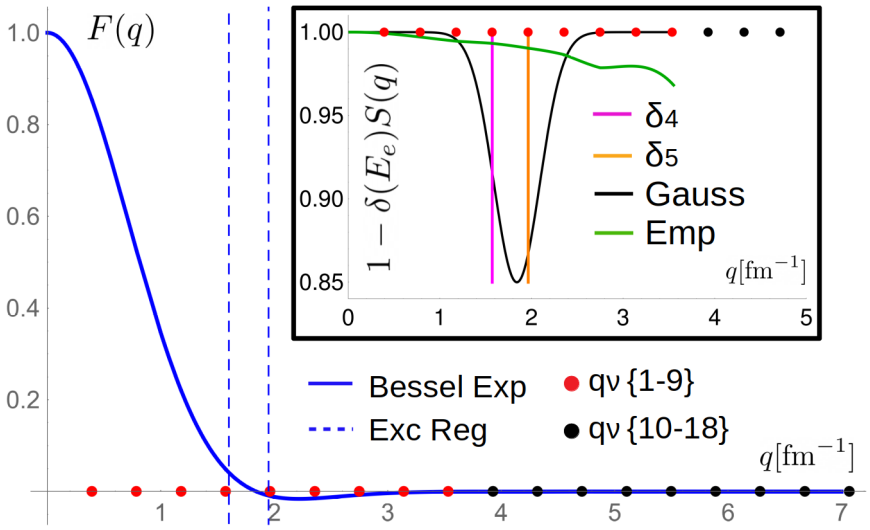

Figure 3: ^{12}C form factor expanded in the Bessel functions formalism using Offermann [5] coefficients without dispersive corrections. The circles in the q axis shows the special values of momentum transfer for the first 9 (red) from experimental data and the second 9 (black) from the extrapolation suggested in [35]. The dashed blue lines encloses the region of the data excluded from the analysis in [5]. The inset plot shows the three test forms for $S(q)$ in addition to the empirical perturbation obtained directly from the data by third degree spline interpolation. The curves in the inset plot are the ones needed to obtain the corrected $F_{\rm ch}^{stat}$ from the observed $F_{\rm ch}^{disp}$ values.

respectively, while Gaussian represents a Gaussian up-shift of amplitude 1 at its peak (e.g., once again 15% when multiplied by 1/2 $\delta(E_e)$), centered at the diffraction minimum $q = 1.84$ fm^{-1} and with a standard deviation of 0.25 fm^{-1}. An overall up-shift in the form factor was chosen based on the calculations shown on Fig. 2 (right panel), which predict an up-shift in the observed cross sections due to the dispersive effects, which means $\sigma_{disp} \geq \sigma_{stat}$.

The empirical perturbation was obtained as $\delta_{emp}(q_\nu) = [F^*_{disp}(q_\nu) - F^*_{stat}(q_\nu)]/F^*_{stat}(q_\nu)$, where $F^*_{disp}(q_\nu)$ ($F^*_{stat}(q_\nu)$) represents the form factor values obtained from the second (third) column in Table X of [5]. Since no amplitude $\delta(E_e)$ was involved in the empirical perturbation, the value of β cannot be defined and we have:

$$F_{disp}(q_\nu) = F(q_\nu)_{stat}[1 + \delta_{emp}(q_\nu)]. \tag{21}$$

Therefore, while the fits parameters from Fig. 2 (left panel) imply corrections expected to be around 30% on the cross section at 1 GeV for ^{12}C, the effect on the nuclear charge radius from our test calculations is around a percent. A detailed analysis of the impact of dispersive effects on nuclear radii was performed by Offermann et al. [5]: the result is a net relatively small effect of 0.28%, implying a renormalization of the charge distribution to offset the change in the cross section.

When using the empirical perturbation for the δy_i in Eq. (18) we obtain an effect of 0.25% in the radius, very close to the actual 0.26% (reported as 0.28% when using rounded values for the radii) in [5]. It seems that the strength (30%) of the other three perturbations is too big to reproduce the small change in the radius, which might indicate that the effects *on the available data* of the dispersive corrections are roughly at least a factor of five smaller outside the vicinity of the difraction minimum.

The Coulomb field extracted from $\langle r^2 \rangle^{1/2}$ should then also be modified from

$$\mid V_C \mid \;=\; \mid V_C^{stat} \mid \;=\; \frac{KZ}{\langle r^2 \rangle^{1/2}} \; ; K = 1/4\pi\varepsilon_0 \tag{22}$$

to

$$\mid V_C^{disp} \mid \;=\; \mid V_C^{stat} \mid /[1 + \beta\delta(E_e)] \tag{23}$$

As mentioned previously, Coulomb corrections are expected to be comparatively small for GeV energies: $S_{HOB} = 2.6\%$ for a 1 GeV incident electron beam on a ^{208}Pb target. In the remainder of this section, we will assume that the energy dependent correction is solely rising from dispersive corrections and is embedded in the term $\delta_{disp}(E_e)$.

In order to estimate the corrections for ^{208}Pb, we scale the carbon value using Coulomb fields from [7]:

- The scaling is first calculated from the super ratio:

$$R_{\text{scale}} = \frac{V_{C,^{208}\text{Pb}} = 18.5 \text{ MeV}}{V_{C,^{12}\text{C}} = 5.0 \text{ MeV}} \frac{Z_{^{12}\text{C}} = 6}{Z_{^{208}\text{Pb}} = 82} = 26.34\% \tag{24}$$

  Thus giving a value for the dispersive corrections of $26.34\% \times 30\% \simeq 8\%$ that is compatible with the $\sim 6\%$ effect observed by Breton et al. [4].

- The effect on the lead radius can then be obtained by applying the above scaling to the value from Offermann et al. [5]

$$0.28\% R_{\text{scale}} = 0.07\%. \tag{25}$$

  The reported experimental value of the charge radius of lead is [37] $R_{\text{ch}} = 5.5012(13)$ fm which would imply an upward shift to 5.5053(13) fm when taking the 0.07% scaling into account.

The situation is far more complex for parity-violating experiments [30, 31, 38] from which the measured asymmetry is used to extract a neutron skin. These experiments typically occurred near diffractive minima to maximize their sensitivity to the physics [39], where also dispersive corrections contribute the most. Our estimation suggests the importance of this correction for high precision determinations of the radius and/or the neutron skin of heavy nuclei.

It is clear one should take dispersive effects into account; however, to our knowledge, there is no known measurements of dispersive effects using polarized beams and/or target. Therefore, measurements of the energy dependence for dispersive effects using polarized elastic scattering on various nuclear targets ($A > 1$) should be performed to provide an accurate information about the size of these effects in and outside minima of diffraction.

5. Possible effects on the Coulomb Sum Rule

The Coulomb Sum Rule (CSR) [40] is defined as the integral of the longitudinal response function $R_L(\omega, |\mathbf{q}|)$ extracted from quasi-elastic electron scattering:

$$S_L(|\mathbf{q}|) = \int_{\omega>0}^{|\mathbf{q}|} \frac{R_L(\omega, |\mathbf{q}|)}{ZG_{E_p}^2(Q^2) + NG_{E_n}^2(Q^2)} d\omega \tag{26}$$

where $-Q^2 = \omega^2 - \vec{q}^2$ with ω the energy transfer and $\vec{q}$ the three-momentum transfer. $G_{E_{p,n}}(Q^2)$ is the proton (neutron) form factor which reduces to the Sachs electric form factor if the nucleon

is not modified by the nuclear medium [41]. $\omega > 0$ ensures that the integration is performed above the elastic peak. In essence, CSR states that by integrating the longitudinal strength over the full range of energy loss ω at large enough momentum transfer q, one should get the total charge (number of protons) of a nucleus.

The quenching of CSR has been found to be as much as 30% [32] for medium and heavy nuclei. Using a quantum field-theoretic quark-level approach which preserves the symmetries of quantum chromodynamics, as well as exhibiting dynamical chiral symmetry breaking and quark confinement, the most recent calculation by Cloet et al. [42] confirmed the dramatic quenching of the Coulomb Sum Rule for momentum transfers $|q| \gtrsim 2.5$ fm^{-1} that lies in changes to the proton Dirac form factor induced by the nuclear medium.

As previously noted, the nuclear charge distribution $\rho_{\rm ch}(r)$ may be considered as a result from folding the distribution $\rho_{\rm nuc}(r)$ of the nucleons in the nucleus with the finite extension of the nucleons $\rho_p(r)$ [35] as represented in Fig. 4.

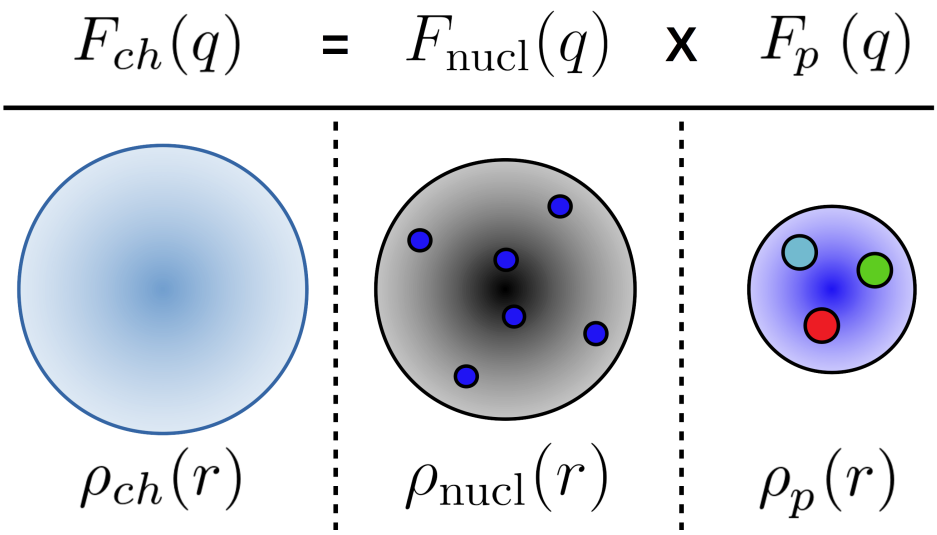

Figure 4: Relationship between the charge, nucleons (protons) and the single proton form factors along with their respective densities for ^{12}C. The protons density $\rho_{\rm nucl}$ specifies the spatial distribution of the 6 protons inside the ^{12}C nucleus, treating them as point particles (blue circles over the black background in the middle column). The charge form factor F_{ch}, which relates to the *charge* distribution in the nucleus (left column), is the result of folding the protons form factor $F_{\rm nucl}$ with the single proton form factor F_p, which relates to the charge distribution inside the proton (right column, the color circles represents the three quarks).

Quasi-elastic electron scattering corresponds to a process in which electrons elastically scattered off nucleons. The nuclear response is affected by the fact that nucleons are not free and carry a momentum distribution, the existence of nucleon-nucleon interactions and interactions between the incoming and outgoing probe and recoils. Therefore, noting that R_L probes $\rho_{\rm nuc} = \rho_{\rm protons}$ while elastic scattering experiments probe $\rho_{\rm ch}(r)$, any measured shift of $F_{ch}(q)$ results from a change in $F_{\rm nuc}$ or F_p, or both. Even when considering the contribution from two-photon exchanges that are responsible for the measured deviation between unpolarized and polarized electron scattering in the extraction of the $\mu G_E^p/G_M^p$ ratio and also believed to be at the origin of the proton form factor puzzle [15] (see the Introduction section), the discrepancy observed cannot explain the 30% quenching of R_L [21, 22, 23]. In the following, we assume that the contribution from dispersive effects found in $\rho_{\rm ch}(r)$ translates entirely in a change in $\rho_{\rm protons}$ and hence in the CSR.

From our naive model (with nuc = p or n):

$$G^{disp}_{E_{\rm nuc}}(Q^2) = \frac{G^{stat}_{E_{\rm nuc}}(Q^2)}{1+\beta\delta(E_e)} \tag{27}$$

Hence:

$$S^{disp}_L(|\mathbf{q}|) = S^{stat}_L(|\mathbf{q}|) \ \times \ [1+\beta\delta(E_e)] \tag{28}$$

Using Fig. 2 for a 600 MeV incident beam on ^{12}C, one would expect a 15% correction in the minimum of diffraction, which is a factor of 7.5 from the 2% prediction from Friar and Rosen [25]. Above the minimum, their prediction indicates an almost linear increase of the dispersion corrections up to about 3.3 fm^{-1} where it reaches a maximum of about 3%. Assuming the same scaling, that is a $0.03 \times 7.5 \simeq 22\%$ predicted effect in the kinematic regime of the CSR data for ^{12}C [43].

Dispersion corrections could have a significant contribution on the Coulomb Sum Rule quenching if the experimentally measured longitudinal response function $R_L(\omega, |\mathbf{q}|)$ is corrected for these effects.

6. Summary

Using a general theoretical framework that allows to propagate the dispersive correction effects, treated as a perturbation, to the coefficients of a Bessel function fit of the form factor, the authors in [1] benchmarked their calculation using the experimental data on ^{12}C from Offermann et al. [5]. They then investigated the impact of these corrections on the nuclear charge density radius and obtained comparable results with the ones reported by the authors. Using scaling arguments, the contribution was found to be around 0.07% for the recent measurement of the nucleon radii from Pb [30, 31, 38], although it will take a detailed investigation and theory to understand how this affects the parity-violating asymmetry. A subsequent study on the observed quenching of the Coulomb Sum Rule [42] indicates that the expected contribution seems to be larger.

The authors in [1] concluded that it was important that a systematic study of the dispersion corrections inside and outside diffraction minima for a large range of (light through heavy) nuclei be performed using both unpolarized and polarized beams/targets to help provide a more complete understanding of elastic (and inelastic) electron/positron-nucleus scattering.

B. Letter of Intent

We are submitting this Letter Of Intent to present the case to measure the energy dependence of the dispersive effects through electron and positron inclusive A(e, e′) elastic scattering around the first diffraction minimum of several nuclei (^{12}C, ^{13}Al, ^{29}Cu, ^{48}Ca, ^{56}Fe, and ^{208}Pb) with five incident beam energies of 0.55, 1.1, 2.2, 3.3 and 4.4 GeV. **These measurements will consist of the first ever comprehensive study of the energy dependence of these effects.**

The experiment could be performed in either the experimental Hall A (using one of the two HRS spectrometers) or Hall C (using the HMS or SHMS spectrometer) at Jefferson Lab in normal configuration with their standard detector systems. Note that few experiments are requesting non-standard CEBAF energies such as 0.7, 1.4, and 2.1 GeV for the PRad-II Collaboration [44] and XXX for the Super-Rosenbluth experiment [45]. The latter has flexibility in terms of the exact beam energies with the goal of having good baseline measurements for $E_{\rm inc} < 1$ GeV and good coverage of the $E_{\rm inc} > 1$ GeV where the difference between the projections is large. Similarly, the

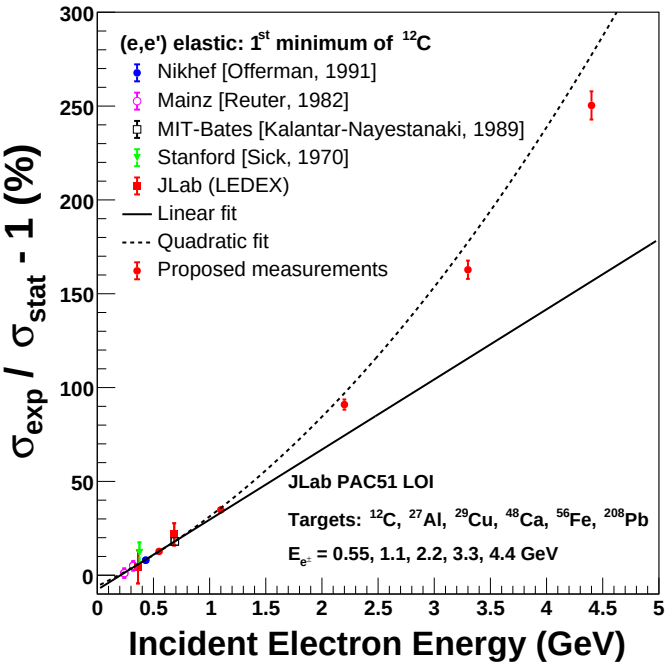

Figure 5: The projected A(e, e′) measurements for 0.55, 1.1, 2.2 3.3 and 4.4 GeV incident electron/positron beam energies.

choice of our beam energies can be modified as one of the primary focus is to perform an energy scan from the sub-GeV regime. While working on our full proposal, we plan to consider the possibility for both our proposed experiment and the Super-Rosenbluth experiment [45] to run together to optimize and reduce the total number of linac settings while still covering the needed beam energies for both measurements. We plan to perform further investigations via Monte Carlo simulation to assess the feasibility of such experiment in Hall A or Hall C.

References Cited

[1] P. Gueye, A. Kabir, P. Giuliani, J. Glister, B. Lee, R. Gilman, D. Higinbotham, E. Piasetzky, G. Ron, A. Sarty, W. Armstrong, J. Arrington, Z.-E. Meziani, and P. Solvignon. Dispersive corrections in elastic electron-nucleus scattering: An investigation in the intermediate energy regime and their impact on the nuclear matter. *European Physical Journal A: Hadrons and Nuclei*, 56(5):– , 126, May 2020. 10.1140/epja/s10050-020-00135-7.

[2] L. S. Cardman, J. W. Lightbody, S. Penner, S. P. Fivozinsky, X. K. Maruyama, W. P. Trower, and S. E. Williamson. The charge distribution of 12 C. *Phys. Lett.*, 91B:203–206, 1980.

[3] E.A.J.M. Offermann, L.S. Cardman, H.J. Emrich, G. Fricke, C.W. deJager, H. Miska, D. Rychel, and H. deVries. Search for Dispersive Effects in Elastic Electron Scattering From ^{12}C. *Phys. Rev. Lett.*, 57:1546–1549, 1986.

[4] V. Breton et al. High accuracy comparison of electron and positron scattering from nuclei. *Phys. Rev. Lett.*, 66:572–575, 1991.

[5] E. A. J. M. Offermann, L. S. Cardman, C. W. de Jager, H. Miska, C. de Vries, and H. de Vries. Energy dependence of the form-factor for elastic electron scattering from C-12. *Phys. Rev.*, C44:1096–1117, 1991.

[6] P. Gueye et al. Dispersive effects from a comparison of electron and positron scattering from C-12. *Phys. Rev.*, C57:2107–2110, 1998.

[7] P. Gueye et al. Coulomb distortion measurements by comparing electron and positron quasielastic scattering off C-12 and Pb-208. *Phys. Rev.*, C60:044308, 1999.

[8] I. Sick and J. S. Mccarthy. Elastic electron scattering from c-12 and o-16. *Nucl. Phys.*, A150:631–654, 1970.

[9] Pierre A. M. Guichon and M. Vanderhaeghen. How to reconcile the Rosenbluth and the polarization transfer method in the measurement of the proton form-factors. *Phys. Rev. Lett.*, 91:142303, 2003.

[10] P. G. Blunden, W. Melnitchouk, and J. A. Tjon. Two photon exchange and elastic electron proton scattering. *Phys. Rev. Lett.*, 91:142304, 2003.

[11] Michail P. Rekalo and Egle Tomasi-Gustafsson. Polarization observables in the processes p+ p —¿ Theta+ + Sigma+ and n+ p —¿ Theta+ + Lambda0, for any spin and parity of the Theta+ hyperon in the threshold region. *Eur. Phys. J.*, A22:119–124, 2004.

[12] Y. C. Chen, A. Afanasev, S. J. Brodsky, C. E. Carlson, and M. Vanderhaeghen. Partonic calculation of the two photon exchange contribution to elastic electron proton scattering at large momentum transfer. *Phys. Rev. Lett.*, 93:122301, 2004.

[13] Andrei V. Afanasev and N. P. Merenkov. Large logarithms in the beam normal spin asymmetry of elastic electron-proton scattering. *Phys. Rev.*, D70:073002, 2004.

[14] J. Arrington. Extraction of two-photon contributions to the proton form-factors. *Phys. Rev.*, C71:015202, 2005.

[15] P. G. Blunden, W. Melnitchouk, and J. A. Tjon. Two-photon exchange in elastic electron-nucleon scattering. *Phys. Rev.*, C72:034612, 2005.

[16] P. G. Blunden and W. Melnitchouk. Dispersive approach to two-photon exchange in elastic electron-proton scattering. *Phys. Rev.*, C95(6):065209, 2017.

[17] D. Adikaram et al. Towards a resolution of the proton form factor problem: new electron and positron scattering data. *Phys. Rev. Lett.*, 114:062003, 2015.

[18] I. A. Rachek et al. Measurement of the two-photon exchange contribution to the elastic $e^{\pm}p$ scattering cross sections at the VEPP-3 storage ring. *Phys. Rev. Lett.*, 114(6):062005, 2015.

[19] B. S. Henderson et al. Hard Two-Photon Contribution to Elastic Lepton-Proton Scattering: Determined by the OLYMPUS Experiment. *Phys. Rev. Lett.*, 118(9):092501, 2017.

[20] D. Rimal et al. Measurement of two-photon exchange effect by comparing elastic $e^{\pm}p$ cross sections. *Phys. Rev.*, C95(6):065201, 2017.

[21] Carl E. Carlson and Marc Vanderhaeghen. Two-Photon Physics in Hadronic Processes. *Ann. Rev. Nucl. Part. Sci.*, 57:171–204, 2007.

[22] J. Arrington, P. G. Blunden, and W. Melnitchouk. Review of two-photon exchange in electron scattering. *Prog. Part. Nucl. Phys.*, 66:782–833, 2011.

[23] A. Afanasev, P. G. Blunden, D. Hasell, and B. A. Raue. Two-photon exchange in elastic electron–proton scattering. *Prog. Part. Nucl. Phys.*, 95:245–278, 2017.

[24] Andreas Aste, Cyrill von Arx, and Dirk Trautmann. Coulomb distortion of relativistic electrons in the nuclear electrostatic field. *Eur. Phys. J.*, A26:167–178, 2005.

[25] James Lewis Friar and M. Rosen. Dispersion corrections to elastic electron scattering by c-12 and o-16. 2. on the use of the closure approximation. *Annals Phys.*, 87:289–326, 1974.

[26] Marco Traini. Coulomb distortion in quasielastic (e, e-prime) scattering on nuclei: Effective momentum approximation and beyond. *Nucl. Phys.*, A694:325–336, 2001.

[27] R. Gilman, D. W. Higinbotham, X. Jiang, A. Sarty, and S. Strauch. LEDEX: Low Energy Deutron EXperiments E05-044 and E05-103 at Jefferson Lab, 2015.

[28] Al Alim Kabir. *Determination of the charge raddi of several light nuclei from precision, high-energy electron elastic scattering.* PhD thesis, Kent State University, Kent State, Ohio, 12 2015.

[29] N. Kalantar-Nayestanaki, C. W. De Jager, E. A. J. M. Offermann, H. De Vries, L. S. Cardman, H. J. Emrich, F. W. Hersman, H. Miska, and D. Rychel. Energy Dependence of Dispersive Effects in ^{12}C. *Phys. Rev. Lett.*, 63:2032–2035, 1989.

[30] C. J. Horowitz et al. Weak charge form factor and radius of 208Pb through parity violation in electron scattering. *Phys. Rev.*, C85:032501, 2012.

[31] S. Abrahamyan et al. Measurement of the Neutron Radius of 208Pb Through Parity-Violation in Electron Scattering. *Phys. Rev. Lett.*, 108:112502, 2012.

[32] J. Morgenstern and Z. E. Meziani. Is the Coulomb sum rule violated in nuclei? *Phys. Lett.*, B515:269–275, 2001.

[33] H. de Vries, C. W. de Jager, and C. de Vries. Nuclear Charge-Density-Distribution Parameters from Electron Scattering. *Atomic Data and Nuclear Data Tables*, 36:495, 1987.

[34] I. Sick. Model-independent nuclear charge densities from elastic electron scattering. *Nuclear Physics A*, 218(3):509 – 541, 1974.

[35] B. Dreher, J. Friedrich, K. Merle, H. Rothhaas, and G. Lührs. The determination of the nuclear ground state and transition charge density from measured electron scattering data. *Nuclear Physics A*, 235(1):219 – 248, 1974.

[36] CODATA18. Committee on data international science council, 2018 codata recommended values, 2018.

[37] I. Angeli and K.P. Marinova. Table of experimental nuclear ground state charge radii: An update. *Atomic Data and Nuclear Data Tables*, 99(1):69 – 95, 2013.

[38] S. Abrahamyan et al. New Measurements of the Transverse Beam Asymmetry for Elastic Electron Scattering from Selected Nuclei. *Phys. Rev. Lett.*, 109:192501, 2012.

[39] J. Piekarewicz, A. R. Linero, P. Giuliani, and E. Chicken. Power of two: Assessing the impact of a second measurement of the weak-charge form factor of ^{208}Pb. *Phys. Rev. C*, 94:034316, Sep 2016.

[40] K. W. McVoy and L. Van Hove. Inelastic Electron-Nucleus Scattering and Nucleon-Nucleon Correlations. *Phys. Rev.*, 125:1034–1043, 1962.

[41] J. V. Noble. Modification of the nucleon's properties in nuclear matter. *Phys. Rev. Lett.*, 46:412–415, 1981.

[42] Ian C. Cloët, Wolfgang Bentz, and Anthony W. Thomas. Relativistic and Nuclear Medium Effects on the Coulomb Sum Rule. *Phys. Rev. Lett.*, 116(3):032701, 2016.

[43] P. Barreau et al. Deep Inelastic electron Scattering from Carbon. *Nucl. Phys.*, A402:515–540, 1983.

[44] A. Gasparian, H. Gao, D. Dutta, N. Liyanage, E. Pasyuk, D. W. Higinbotham, C. Peng, K. Gnanvo, W. Xiong, X. Bai, and the PRad collaboration. Prad-ii: A new upgraded high precision measurement of the proton charge radius, 2020.

[45] J. Arrington. Super-rosenbluth experiment, XXXX.